PROF. JANUSZ NOWOTNY (Orcid ID : 0000-0002-1822-7508)

Author Manuscript

Article type : Article

EC-Ta-TiO_2-2

Corresponding author mail id:J.Nowotny@uws.edu.au

Electrical Conductivity and Defect Disorder of Tantalum Doped TiO_2

Mohammad A. Alim[1], Tadeusz Bak[1], Armand Atanacio[2], Johan Du Plessis[2], Meifang Zhou[3], Joel Davis[4] and Janusz Nowotny[1]

1. *Solar Energy Technologies, School of Computing, Engineering and Mathematics, Western Sydney University, Locked Bag 1797, Penrith, NSW 2751, Australia*
2. *School of Applied Sciences, RMIT University, City Campus, Melbourne, VIC 3001, Australia*
3. *School of Chemistry, The University of Melbourne, Parkville, Melbourne, VIC 3010, Australia.*
4. *Australian Nuclear Science and Technology Organisation, Locked Bag 2001, Kirawee, DC, NSW 2232, Australia*

Abstract

The present work reports the electrical properties of polycrystalline Ta-doped TiO_2 (0.39 at.% Ta) determined *in situ* at elevated temperatures (1173 K - 1323 K) in the gas phase of controlled oxygen activity (10^{-12} Pa to 10^{4} Pa). The effect of oxygen activity on the electrical

This is the author manuscript accepted for publication and has undergone full peer review but has not been through the copyediting, typesetting, pagination and proofreading process, which may lead to differences between this version and the Version of Record. Please cite this article as doi: 10.1111/jace.14959

This article is protected by copyright. All rights reserved

conductivity and thermoelectric power of TiO_2 is discussed in terms of defect disorder, including (1) the intrinsic electronic disorder that is governed by electronic compensation in the strongly reducing regime, (2) the extrinsic electronic disorder that is governed by electronic charge compensation in the reducing regime and (3) the extrinsic ionic disorder that is governed by ionic compensation in the oxidising regime. It is shown that tantalum ions are incorporated into the titanium sublattice of TiO_2 leading to the formation of donor-type energy levels. The Arrhenius-type plot of the electrical conductivity data leads to the determination of the formation enthalpy terms. The obtained results are considered in terms of the effect of tantalum and oxygen activity on the defect disorder and the associated key performance-related properties in the light-induced partial water oxidation.

1. Introduction

Titanium dioxide is the promising material for water oxidation using solar energy [1-5]. This process, leading either to partial or total water oxidation, may be applied in water purification and the generation of solar fuel, respectively. Intensive research aims at processing TiO_2 with enhanced performance in these applications.

The most commonly applied research strategy in processing TiO_2 with enhanced performance is based on the incorporation of a range of extrinsic ions into the TiO_2 lattice [2-5]. The influence of the extrinsic ions on the performance in solar energy conversion by TiO_2 has been commonly considered to be determined by reduction of the band gap, which leads to enhanced absorption of sunlight. While the effect of the band gap on light absorption is obvious, the recent studies show that the solar-to-chemical energy conversion by oxide semiconductors and the related charge transfer is profoundly influenced by a range of the key performance-related properties, KPPs, such as the concentration of surface active sites, charge transport, Fermi level and the band gap [5-7]. It is shown that the KPPs are defect related. For example titanium vacancies are the anodic active sites for water oxidation [5-7]. Therefore, these can be modified by defect engineering [5-7].

The present work, which is part of a larger research program on the effect of KPPs of TiO_2 on the solar-to-chemical energy conversion, is the determination of the effect of tantalum on the semiconducting properties and the related defect disorder of TiO_2. The studies are performed using the measurements of the electrical properties, which are sensitive to defect disorder, such as electrical conductivity and thermoelectric power. These electrical properties are used

This article is protected by copyright. All rights reserved

Author Manuscript

for *in situ* monitoring the defect disorder during processing at elevated temperatures in order to determine the optimal conditions of the processing procedure that leads to enhanced performance.

The experimental part of this work is preceded by definition of terms and a brief overview of the literature on the effect of donor-type ions, such as tantalum and niobium, on the electrical properties of titanium dioxide.

2. Definitions of Terms

2.1 Defect Disorder of Pure and Tantalum-Doped TiO_2

The intrinsic ionic defects that have an impact on properties of TiO_2 include oxygen vacancies, titanium vacancies and titanium interstitials as well as electronic defects (electrons and electron holes). The formation/removal of these defects may be represented by appropriate defect reactions and the related charge neutrality conditions, which are shown in **Table 1** (the most convenient representation of defect reactions is by using the Kröger-Vink notation [8] that allows the formulation of the charge neutrality conditions relatively easy).

Table 1. Defect equilibria, the related equilibrium constants and the associated standard enthalpy and entropy of defect formation (n and p represent the concentration of electrons and electron holes, respectively, and square brackets denote concentrations)

The mechanism of tantalum and niobium incorporation into the TiO_2 lattice and the related charge neutrality depends on oxygen activity during processing [9, 10]. In reducing conditions tantalum has the tendency to enter the titanium lattice sites leading to the formation of singly charged ions and quasi-free electrons as represented by the following reaction:

$$Ta_2O_5 \rightarrow 2Ta_{Ti}^{\bullet} + 2e' + 4O_O^x + \frac{1}{2}O_2 \qquad (1)$$

The charge neutrality requires that the positive charge of the tantalum ions is compensated by electrons:

$$n = \left[Ta_{Ti}^{\bullet}\right] \qquad (2)$$

Author Manuscript

This article is protected by copyright. All rights reserved

The mechanism (1) may be attested by the measurements of the electrical conductivity. If the mobility term is independent of oxygen activity, the changes of the electrical conductivity are directly proportional to the concentration of tantalum. However, when processing occurs in oxidising conditions, the formation of positively charged tantalum ions in the titanium site is compensated by negatively charged titanium vacancies:

$$2Ta_2O_5 \rightarrow 4Ta_{Ti}^{\bullet} + V_{Ti}^{''''} + 10O_O^x \qquad (3)$$

Then the charge neutrality condition of this reaction requires that:

$$4\left[V_{Ti}^{''''}\right] = \left[Ta_{Ti}^{\bullet}\right] \qquad (4)$$

Application of the mass action law to reaction (4) in Table 1, at the condition (4), results in the following expression for the concentration of electrons:

$$n = \left(\frac{K_i^{\,4}\left[Ta_{Ti}^{\bullet}\right]}{4K_4}\right)^{1/4} p\left(O_2\right)^{-1/4} \qquad (5)$$

As seen, in this case the concentration of electrons depends on the content of tantalum and oxygen activity with the exponent of -1/4. If the mobility term is independent of oxygen activity, then the slope of the $\partial\log\sigma$ as a function of $\partial\log p(O_2)$ is equal -1/4 (where σ is the electrical conductivity, the square brackets denotes concentrations and the remaining parameters are defined in Table 1).

When oxygen activity is extremely low and the concentration of electrons generated by ionisation of the intrinsic defects becomes substantially larger than that required for the condition (2), then the excess of electrons is compensated by oxygen vacancies, which become the predominant defects of TiO_2. Then the charge compensation requires that:

$$n = 2\left[V_O^{\bullet\bullet}\right] \qquad (6)$$

Author Manuscript

This article is protected by copyright. All rights reserved

Application of the mass action law to the reaction (1) in Table 1 and the conditions (6) results in the following dependence:

$$n = (2K_1)^{1/3} p(O_2)^{-1/6} \tag{7}$$

The electrical effects related to the relations (1) – (7) may be used for derivation of an isothermal representation of the effect of oxygen activity on the concentration of both electronic and ionic defects in terms of so called Brouwer-type diagram, which is represented in **Figure 1**. The fraction numbers in Figure 1 are related to the oxygen exponent is related to 1/m associated with electrons or electron holes:

$$\frac{1}{m_{n,p}} = \frac{\partial \log(n, p)}{\partial \log p(O_2)} \tag{8}$$

Figure 1. The Brouwer-type diagram for Ta-doped TiO_2 showing defect disorder within different ranges of oxygen activity (where square brackets denote concentrations and the fraction numbers are represented by Equation (8)

As seen, the slope of the effect of oxygen activity on the concentration of electrons demarcates the following three regimes of the defect disorder for Ta-doped TiO_2:

1. Regime I. In this regime the slope of log n vs. log $p(O_2)$ is governed by Equation (7).
2. Regime II. This regime is governed by the condition (2).
3. Regime III. The slope of log n vs. log $p(O_2)$ in this regime is governed by Equation (5).

The boundary values of oxygen activity corresponding to the limits of the Regime II may be determined by the measurements of the electrical conductivity assuming that the mobility term is independent of oxygen activity [10]. This is one of the aims of the present work.

2.2 Electrical Conductivity

The electrical conductivity, σ, is the product of both the concentration and the mobility terms:

$$\sigma = en\mu_n \tag{9}$$

Author Manuscript

This article is protected by copyright. All rights reserved

where e is the elementary charge and μ_n is the mobility term. Assuming that the mobility is independent of oxygen activity the electrical conductivity may be represented as a function of oxygen activity in the following form:

$$\frac{1}{m_\sigma} = \frac{\partial \log \sigma}{\partial \log p(O_2)} \tag{10}$$

where $1/m_\sigma$ is the $p(O_2)$ exponent, which is the parameter that may be used for the verification of specific defect models.

The relations (1) – (10) are derived for isothermal conditions. Description of the effect of temperature on defect disorder and the related properties is more complex since both the concentration and the mobility terms depend on temperature. Taking into account that both electrical conductivity terms are activated, these may be represented as:

$$\mu_n = const.\exp\left(-\frac{\Delta H_m}{RT}\right) \tag{11}$$

$$n = const.p(O_2)^{\frac{1}{m}} \exp\left(-\frac{\frac{2}{m}\Delta H_f}{RT}\right) \tag{12}$$

where the parameter *const* in Equations (11) and (12) includes equilibrium constants, ΔH_m is the activation enthalpy of motion of electrons, m is the parameter related to the ionisation degree of defects and ΔH_f is the enthalpy of the formation of defects. Therefore, the effect of temperature on electrical conductivity can represented as:

$$\sigma = const.\exp\left(-\frac{\frac{2}{m}\Delta H_f + \Delta H_m}{RT}\right) \tag{13}$$

where the activation energy term is:

$$\Delta E_\sigma = \frac{2}{m}\Delta H_f + \Delta H_m \tag{14}$$

Author Manuscript

This article is protected by copyright. All rights reserved

The enthalpy term may be determined from the activation energy of the electrical conductivity, when the mobility term is known.

2.3. Thermoelectric Power

Thermoelectric power, S, is the ratio of thermoelectric voltage, ΔΨ, which is formed along a temperature gradient, to the related temperature difference, ΔT:

$$S = \frac{\Delta\Psi}{\Delta T} \tag{15}$$

The thermoelectric power can be related to the concentration of electrons and holes within the n- and p-type regimes, respectively:

$$S_n = \frac{k}{e}[\ln\frac{N_n}{n} + A_n] \tag{16}$$

$$S_p = \frac{k}{e}[\ln\frac{N_p}{p} + A_p] \tag{17}$$

where N is the density of states, A is the kinetic constant and the subscripts n and p are related to electrons and holes. Knowledge of the thermoelectric power allows the determination of the Fermi level, E_F. For pure n-type regime, the E_F is related to thermoelectric power according to the following expression:

$$S_n = \frac{E_F - E_C}{eT} - \frac{k}{e}A_n \tag{18}$$

where E_C is the bottom of the conduction band.

The effect of oxygen activity on the thermoelectric power may be represented by the following relation:

$$\frac{1}{m_S} = \frac{k}{e}\frac{\partial S}{\partial \log p(O_2)} \tag{19}$$

where $1/m_S$ can be related to defect disorder.

Author Manuscript

This article is protected by copyright. All rights reserved

3. Brief Literature Overview

There has been common perception that the band gap is the key property of semiconductors that has the critical effect on the efficiency of solar-to-chemical energy conversion [2-4, 11-16]. Therefore, the research strategy on the development of TiO_2-based systems with enhanced performance is focused on reduction of the band gap.

On the other hand, recent study by Bak et al. [5] reveals that alternative properties such as, surface active sites, charge transport, charge transfer, Fermi level and flat band potential, may also have a profound influence on photocatalytic performance of TiO_2 in addition to the band gap. It has been documented that all these key performance-related properties (KPPs) are closely related to the concentration of lattice imperfection [5-7]. Therefore, the properties of TiO_2-based semiconductors can be enhanced by defect engineering [17].

Since the effect of tantalum on properties of TiO_2 is very similar to that of niobium, this overview includes the reports related to the effect of both tantalum and niobium on the electrical [18-21], photocatalytic [11-16], photovoltaic [22, 23] as well as alternative properties [24-26]. Since the effect of the extrinsic ions, such as tantalum and niobium, on properties of TiO_2 is also affected by oxygen, the present work considers the determination of the effect of oxygen activity on the electrical properties.

The properties of solid solutions are well defined when the concentration of the solute ions is within the solubility limit. This limit is approximately 4-8 at% for tantalum [27] and 8-18 at% of niobium [9].

There is a common perception that the pentavalent ions, such as tantalum and niobium, are incorporated into the TiO_2 lattice according to the substitutional mechanism [9, 10, 18-21]. Comini et al [25] observed that addition of niobium or tantalum to the anatase phase of TiO_2 results in the transition of anatase to rutile. Since the rutile phase is the only stable TiO_2 phase at elevated temperatures, effect reported by Comini et al is essential mainly at lower temperatures.

Balachandran and Eror [24] reported that up to 10 at. % tantalum in Ta-doped TiO_2 can be compensated within a single phase by intrinsic defects. In strongly reducing conditions the compensation is achieved by the generation of Ti^{3+} ions. In contrast, at high oxygen activities

Author Manuscript

This article is protected by copyright. All rights reserved

an additional uptake of oxygen, which was observed, can be accommodated in the rutile structure by creation of metal deficit-related defects (titanium vacancies) and compensate an excess charge of tantalum.

Extensive studies have been reported on the effect of niobium on the electrical properties of TiO_2 in terms of both electrical conductivity and thermoelectric power measurements in a wide range of temperatures and oxygen activity [19-21]. These studies resulted in the determination of the combined effect of both the extrinsic defects related to niobium and the intrinsic defects on the concentration of electronic charge carriers. The effect is represented schematically in **Figure 2**, showing the isothermal plots of the concentration of electrons, electrical conductivity and thermoelectric power as a function of oxygen activity for donor-doped TiO_2.

Figure 2. Schematic representation of the effect of oxygen activity on the concentration of electrons (a), electrical conductivity (b) and thermoelectric power (S) for donor-doped TiO_2, where D is a donor-type ion (c), the fractions are related to the oxygen activity-related exponent for specific quantities represented by Equations (8), (10) and (18), respectively

Such plots allow the determination of the critical values of oxygen activities corresponding to the transition between the regimes corresponding to different defect disorder.

A range of studies on the effect of niobium on the electrical conductivity of TiO_2 are reported by Baumard and Tani [19-20]. The effect is schematically represented in **Figure 3** showing the log σ vs. log $p(O_2)$ dependence for different concentration of niobium. As seen, pure TiO_2 in strongly reducing conditions exhibits the slope of -1/6. This dependence is observed also for Nb-doped TiO_2 when the oxygen activity is reduced below the level that is required for imposition of the concentration of oxygen vacancies that is competitive with the effect of niobium.

Figure 3. Schematic representation of the effect of oxygen activity for pure and Nb-doped TiO_2 in reducing and strongly reducing conditions [19-20]

Both tantalum and niobium have a substantial effect on photocatalytic properties of TiO_2 [11-16]. These reports, which are contradictory, indicate that the applied procedures in the

Author Manuscript

This article is protected by copyright. All rights reserved

formation of solid solutions are not reproducible. On the other hand, the number of reports on the effect of donor-type doping on electrical properties is limited [18-21]. The reported data require verification on the effect of temperature and oxygen activity on properties. Therefore, the aim of the present work is verification of the reported results using combined determination of two electrical properties determined simultaneously; electrical conductivity and thermoelectric power.

4. Experimental

Specimens

The polycrystalline specimens of Ta-doped TiO_2 were prepared by solid state reaction of TiO_2 (rutile) and Ta_2O_5. The desired compositions were achieved by appropriate stoichiometry of the reactants that were mixed in the ball mill for 2 h and subsequently placed in a tube furnace at 1273 K for 48 h in air. The sintering conditions (time and temperature) were selected based on the diffusion data for niobium and assuming that the diffusion rate for tantalum is similar to that of niobium. The obtained sintered body of Ta-doped TiO_2 was then crushed into fine powder in a ceramic mortar, mixed with paraffin binder and pressed uniaxially in 25 mm diameter die under 50-60 MPa. Then the pellets were isostatically pressed under 400 MPa for 2 min. The paraffin binder was removed by heating at 873 K for 10 h in air. The pellets were sintered at 1673 K for 3 h in air.

Morphology

The SEM micrographs of both pure and Ta-doped TiO_2 after polishing and annealing as well as Ta-doped TiO_2 after the electrical conductivity measurements are shown in **Figure 4**.

Figure 4. The SEM micrographs for (a) pure TiO_2, (b) Ta-doped TiO_2 specimen after polishing and subsequent annealing at 1273 K for 2 h and (c) Ta-doped TiO_2 specimen after all oxidation and reduction runs associated with the electrical conductivity measurements - magnification of 2000

As seen in **Figure 4**, the specimens of pure TiO_2 exhibits high density with the grain size of 5-60 µm. Addition of tantalum results in reduction of the grain size to 2-20 µm. Moreover, the Ta-doped TiO_2 exhibits an insignificant level of porosity. However, the morphology of the Ta-doped TiO_2 after the electrical conductivity measurements is entirely different. In the

Author Manuscript

This article is protected by copyright. All rights reserved

latter case the specimens exhibits a lot of small surface islets, scattered along the surface, which were formed during the prolonged measurements involving both oxidation and reduction experiments.

Bulk Composition

Bulk composition of the studied specimen was determined using the nuclear facility of proton induced X-ray emission, PIXE, which is shown in **Figure 5**.

Figure 5. The PIXE spectra for pure and the Ta-doped TiO_2 (the peaks are related to the indicated elements)

The concentration of specific elements related to different peaks can be determined from the surface areas under the related peaks. The red-line represents the spectrum background that has been used for the determination of the content of the elements. The list of the detected species in the PIXE analysis and the related concentrations for Ta-doped TiO_2 (0.39 at. %) sample are in **Table 2**.

Table 2. The concentration of the elements determined by the PIXE analysis, including the element incorporated intentionally (tantalum) and not-intentionally (contaminations).

As seen in the spectrum of PIXE, which is shown in **Figure 5**, the concentration of intentional dopant (tantalum) in the Ta-doped specimen is 0.39 at%. Table 2 shows that the predominant contamination (unintentional dopant) is chlorine (0.12 at%). Its mechanism of incorporation into the TiO_2 lattice may be represented by the following Equation:

$$Cl_2 \leftrightarrow 2Cl_O^{\bullet} + V_{Ti}^{''''} + 2h^{\bullet} \qquad (20)$$

The chlorine ions are incorporated into the oxygen sites leading to the formation of donors, however, the associated formation of titanium vacancies, which are charged negatively, results in the formation of electron holes. Therefore, the reaction (20) results in compensation of the charge related to the electrons formed as a result of reaction expressed by the reaction (1).

Band Gap

The band gap was determined using the Agilent Cary 5000 UV–vis–NIR spectrophotometer in the mode of diffuse reflectance (DRA-2500). The reflectance spectra were recorded within

Author Manuscript

This article is protected by copyright. All rights reserved

the wavelength range 300−800 nm at the scan rate of 600 nm/min. The spectra were used for the determination of the band gap using the Tauc method [28-30]. The effect of tantalum on the band gap of TiO_2 is in **Figure 6**.

Figure 6. Effect of tantalum concentration on the band gap

As seen, tantalum results in an insignificant increase of the band gap by 0.1 eV. Assuming, however, that tantalum results in the formation of donor levels, which in analogy to Nb-doped TiO_2, are located in the close proximity of the band gap [26], its effect of conduction is essential.

Electrical Properties

The applied electrical circuitry allowed for simultaneous measurements of both the electrical conductivity and thermoelectric power in identical conditions of temperature and oxygen activity. A schematic representation of the experimental circuit and the sample holder is shown in **Figure 7.**

Figure 7. A schematic representation of experimental set-up for the determination of the electrical conductivity using the four probe method (appropriate wiring was provided for the electrical monitoring devices, which were located outside the high temperature area)

As seen, the rectangular shaped Ta-doped TiO_2 specimen is placed between two platinum plates forming current electrodes, which are connected to the current source. A spring mechanism had been employed to maintain the effective galvanic contact between the studied specimen and electrodes. Two platinum wires were wrapped around the middle part of the specimen and connected with the electrometer. The function of these wires, forming voltage probes, is to collect the voltage along the specimen. Two micro-heaters, equipped with thermocouples, were attached at both sides of the sample to impose a temperature gradient, ΔT. The Seeback voltage, ΔV, generated as a result of ΔT was determined using the electrometer. The entire circuitry, including the sample holder, was placed in a tube furnace that was connected with a gas flow system.

The desired oxygen activity in the reaction chamber was imposed by the composition of the gas phase mixture. An electrochemical zirconia probe was used to determine the oxygen activity in the reactor.

Author Manuscript

This article is protected by copyright. All rights reserved

The electrical conductivity was measured as a function of time after a new oxygen activity was imposed on the reaction chamber involving the studied specimen. The electrical conductivity measurements involved two experimental approaches.

In the first approach the electrical conductivity was applied for isothermal *in situ* monitoring the equilibration kinetics during oxidation and reduction experiments. The measurements in this approach were taken at constant DC current, 10 μA, which was applied alternatively in both directions (in order to minimize the polarization effect). The equilibrium state was reached when the electrical conductivity reached a constant value as a function of time. Then the second approach was applied.

The second approach consists in the measurements of both thermoelectric power and the electrical conductivity. In the latter case the electrical conductivity measurement included 10-15 independent voltage readings for different currents applied in both directions (the applied current was in the range of 10 nA - 1 mA in such manner that the overall voltage across the specimen was lower than 5V).

Oxygen Activity

The oxygen activity, $p(O_2)$, was imposed in the reaction compartment by the gas mixtures of appropriate compositions flowing through the reactor. The total flow rate of the gas mixture was 100 ml/min throughout the experiment. Measurements were taken in both oxidizing and reducing environments. The desired oxidizing regimes, in the range of 100 kPa – 10 Pa, were achieved by mixing of argon/oxygen gases in different ratios. The reducing conditions were obtained by the gas mixture of argon, including 1% of hydrogen, and argon without hydrogen. Oxygen activity in reducing condition was in the range between 10^{-15} Pa and 10^{-9} Pa in the studies temperature ranges.

Experimental Procedure

Figure 8 demonstrates a standard monitoring sheet, including the changes of the oxygen activity (Figure 7a), fluctuation of temperature during isothermal experiment corresponding to 1173 K (Figure 7b) and the resulting changes of the electrical conductivity (Figure 4c). As seen, the temperature fluctuations remain within 0.3 K. As also seen, the electrical conductivity reaches the equilibrium state at 1173 K within 20 h.

Author Manuscript

This article is protected by copyright. All rights reserved

Figure 8. The monitoring sheet involving the changes of oxygen activity (a), temperature (b) and the electrical conductivity as a function of time within a single step of the reduction experiment for Ta-doped TiO_2 at 1173 K

The experimental procedure involving isothermal step-wise changes of oxygen activity within successive experiments of reduction (c) and resulting changes of the electrical conductivity (a) and thermoelectric power (b) at 1273 K for Ta-doped TiO_2, are shown in **Figure 9**.

Figure 9. Isothermal changes of (a) the electrical conductivity, (b) thermoelectric power and (c) oxygen activity as a function of time for Ta-doped TiO_2 at 1273 K

The entire cycle of the measurements, involving the equilibration experiments during oxidation and reduction in the studied range 1173 K – 1323 K, and the determination of both electrical conductivity and thermoelectric power (running non-stop), lasted approximately 5 months.

5. Results and Discussion

Effect of Oxygen Activity

The plots of the isothermal changes of the electrical conductivity (determined in equilibrium) as a function of oxygen activity are in **Figure 10**.

Figure 10. Electrical conductivity of Ta-doped TiO_2 (0.39 at. %) as a function of oxygen activity in the temperature range 1173 – 1323 K (dashed lines are the extrapolated dependences)

As seen, the electrical conductivity changes of polycrystalline Ta-doped TiO_2 in the temperature range 1173-1323 K fall into the three regimes as it is the case for Nb-doped TiO_2. Unfortunately, the experimental data in the middle part of the dependence corresponding to the Regime II, which is shown by dashed lines, is derived by extrapolation since the oxygen activities in this regime are not available by the gas flow system applied in this work. However, the extrapolated dependences, derived between the boundary conditions of the Regimes I and III, confirm that the related dependence can be best described by reaction that is governed by the charge neutrality represented by Equation (2). In summary,

Author Manuscript

This article is protected by copyright. All rights reserved

the electrical conductivity data confirm that the defect disorder of Ta-doped TiO_2 may be considered in terms of the following regimes:

- Regime I. This regime, corresponding to the strongly reducing regime, is governed by the charge neutrality expressed by Equation (6) and the related exponent of $p(O_2)$ is $1/m_\sigma = -1/6$.
- Regime II. This regime, corresponding to reducing conditions, is governed by the condition (2). In this regime the electrical conductivity is independent of oxygen activity.
- Regime III. This regime corresponds to the defect disorder model represented by equation (5) that is governed by the charge neutrality condition (4).

The obtained experimental data for Ta-doped TiO_2, compared with the data for pure and Nb-doped TiO_2 [31, 21], are shown in **Figure 11**.

Figure 11. The effect of oxygen activity on the electrical conductivity for pure and Ta-doped TiO_2 (plotted along Nb-doped TiO_2) at (a) 1173 K (the plot for Nb-doped TiO_2 corresponds to 1198 K), 1223 K (b), 1273 K (c) and 1323 K (d)

As seen, the character of the log σ vs. log $p(O_2)$ dependencies for Ta-doped TiO_2 and Nb-doped TiO_2 is very similar within all regimes. Tantalum has a substantial effect on the electrical conductivity within the oxidizing and reducing regimes. The effect of tantalum can be ignored when oxygen activity is reduced below the level corresponding to the strongly reducing regime. Then the defect disorder of both pure Ta-doped TiO_2 and TiO_2 is governed by the intrinsic electronic charge neutrality. Figure 11 shows that the experimental slope of log σ as a function of log $p(O_2)$ has the tendency to merge for both pure and Ta-doped TiO_2. This tendency has been attested experimentally by Baumard and Tani [19] for diluted Nb-doped TiO_2.

Figure 12 compares the electrical conductivity data obtained in the present work with the data reported by Tani and Baumard [18].

Figure 12. Effect of oxygen activity on the electrical conductivity of Ta-doped TiO_2 at 1273 K obtained in this work along the data reported by Tani and Baumard [18]

Author Manuscript

This article is protected by copyright. All rights reserved

As seen, the agreement between the characters of the obtained dependences is outstanding. The difference in absolute values of the electrical conductivity data in the range corresponding to the condition (2) is consistent with the difference of the content of tantalum.

The isothermal changes of thermoelectric power as a function of oxygen activity at 1323 K are shown in **Figure 13**.

Figure 13. The isothermal dependences of the thermoelectric power as a function of oxygen activity for Ta-doped TiO_2 in the range 1173 K – 1323 K

As seen in **Figure 13**, the slope of S vs. log $p(O_2)$, which is similar to that of log σ vs. log $p(O_2)$ within the oxygen activity regimes as it is represented in **Figure 11**, is consistent with the related defect disorders.

Equation (19) may be used in the determination of the Fermi level from the thermoelectric power data in purely n-type regime. This is the case for the thermoelectric power data of Ta-doped TiO_2 in **Figure 13** corresponding to the strongly reducing regime [$p(O_2)<10^{-7}$ Pa] at 1323 K. The resulting Fermi level is represented in **Figure 14** in comparison with the E_F data determined for pure TiO_2 single crystal at the same temperature. The scale in **Figure 14** is reflective of the relative positions of the E_F vs. log $p(O_2)$ plots for pure and Ta-doped TiO_2. However, taking into account that the energy level of niobium is in the close vicinity of the conduction band [26] assuming that the absolute value of the energy level of tantalum is similar to that of niobium, the values on the y-axis can be considered in the first approach as reflective of the distance from the bottom of the conduction band.

Figure 14. Effect of oxygen on the Fermi level of pure and Ta-doped TiO_2 at 1323 K

Figure 14 shows that tantalum results in a substantial increase of the Fermi level, which at 1323 K is approximately 0.15 eV. This effect is consistent with the energy level of niobium in the TiO_2 lattice.

Temperature Dependence

This article is protected by copyright. All rights reserved

Author Manuscript

The effect of temperature on electrical conductivity is shown in **Figure 15** both in reducing (a) and oxidising (b) conditions.

Figure 15. Isobaric Arrhenius plots for Ta-doped TiO_2 in reducing and oxidising conditions

The activation energy exhibits the lowest value (33 kJ/mol) for the reducing regime that is governed by the extrinsic charge neutrality.

As seen in **Figure 16,** the activation energy of the electrical conductivity for Ta-doped TiO_2 in the strongly reducing regime remains in the range of 30-40 kJ/mol for Ta-doped and 1-5 kJ/mol for Nb-doped TiO_2. As also seen the activation energy values in the oxidising regime for both Nb-doped TiO_2 and Ta-doped TiO_2 are similar.

The effect of oxygen activity on the activation energy of the electrical conductivity is shown in **Figure 16** for Ta-doped TiO_2 along with the data for pure TiO_2 and Nb-doped TiO_2. In the calculation of $E_{\sigma,}$ the mobility term, ΔH_m, is considered same as for Nb-doped TiO_2 which is 0.7 kJ/mol [32].

Figure 16. Effect of oxygen activity on the activation energy of electrical conductivity

The activation energy for pure TiO_2 increases with the decrease of oxygen activity showing a tendency to achieve a maximum, at the level of over 215 kJ/mol within the ionic charge compensation regime. Imposition of strongly reducing conditions, governed by the electronic charge compensation, results in the drop of the activation energy to 170 kJ/mol. Reduction of Ta-TiO_2 in oxidising conditions (ionic charge compensation) leads to an insignificant decrease of the activation energy from to the level of 55 kJ/mol to 40 kJ/mol. The effects for Nb-doped TiO_2 are similar. However, the effects of tantalum and niobium on the activation energy in reducing conditions are entirely different.

The activation energy in the two regimes can be considered in terms of the enthalpy of formation. These are shown in **Figure 17**.

Figure 17. The effect of oxygen activity on the enthalpy of defect formation of TiO_2

This article is protected by copyright. All rights reserved

Author Manuscript

The defect formation enthalpy term, determined in equilibrium from the electrical conductivity data for high-purity TiO_2 and Ta-doped TiO_2 in **Figure 16**, is shown in **Figure 17**. In the determination of the ΔH_f term, the following assumptions have been made:

- The parameter m_σ at low and high $p(O_2)$ is 6 and 4, respectively.
- The mobility term is independent of oxygen activity, $p(O_2)$.

As seen in **Figure 17,** the enthalpy term for Ta-doped TiO_2 decreases with decreasing $p(O_2)$ from 100 kJ/mol at 10^5 Pa to 20 kJ/mol at 1 Pa and then increases to 120 kJ/mol at $p(O_2)=10^{-11}$ Pa. The effect of niobium on the ΔH_f term is similar at $p(O_2)>1$ Pa. However, the picture in strongly reducing conditions is entirely different. The enthalpy term, ΔH_f, for Ta-doped TiO_2, which at $p(O_2) = 10^{-11}$ kJ/mol assumes 106 kJ/mol, decreases to 82 kJ/mol at 10^{-9} Pa. As also seen, the effect of oxygen activity on the ΔH_f term for Nb-doped TiO_2 and Ta-doped TiO_2 is entirely different. These results indicate that the oxygen activity corresponding to the boundaries between the defect disorder regimes for tantalum and niobium in the strongly reducing regime are different as well.

6. Conclusions

The obtained experimental results indicate that the defect disorder of Ta-doped TiO_2 is similar to that of Nb-doped TiO_2 in terms of the mechanism of incorporation. Therefore, the defect reactions representing the effect of oxygen activity on defect disorder are essentially the same for both solid solutions.

The difference is associated with the oxygen activities corresponding to the boundaries between different defect disorder regimes. As seen in **Figure 17**, while the defect formation term in oxidising conditions is very similar for both ions, the difference between the two in the strongly reducing conditions is substantial.

The effect of tantalum on defect disorder of TiO_2 may be summarised in terms of the following points:

- The slope of -1/4 for the log σ vs. log $p(O_2)$ plot in oxidising conditions [$p(O_2)>1$ Pa] is consistent with the substitution mechanism of tantalum incorporation leading to the formation of donors.

Author Manuscript

This article is protected by copyright. All rights reserved

- The slope of -1/6 for the log σ vs. log $p(O_2)$ plot in the strongly reducing conditions [$p(O_2) < 10^{-8}$ Pa] indicates that the defect disorder is determined by intrinsic defects and the effect of tantalum, present at the level of 0.39 at%, may be ignored.
- The experimental set-up applied in this work did not allow for imposition of the oxygen activity corresponding to the range 10^{-8} at% < $p(O_2)$ <1 Pa. However, the extreme absolute values of the electrical conductivity and the thermoelectric power corresponding to the neighbouring regimes (the latter are almost identical) indicates that the defect disorder of Ta-doped TiO_2 in reducing conditions is governed by the extrinsic electronic charge compensation.

The electrical properties determined in the present work allow the following points to be made on the effect of the KPPs for the solar-to-chemical energy conversion:

1. The incorporation of tantalum into TiO_2 results in the formation of titanium vacancies, which are the active sites for water adsorption [5-7].
2. Tantalum results in an increase of the electrical conductivity. The effect is most substantial in reducing conditions when tantalum results in defect disorder that is governed by electronic charge compensation. The effect of tantalum on conductivity is less substantial in oxidising regimes when tantalum leads to the defect disorder that is governed by ionic compensation. On the other hand, in this regime tantalum has major effect on the concentration of titanium vacancies. The effect of tantalum on conduction and the concentration of titanium vacancies is least substantial in the strongly reducing regime when defect disorder is governed by the intrinsic charge compensation.
3. Tantalum results in an increase of the Fermi level despite the associated formation of titanium vacancies.

Acknowledgements

The support of the Australian Institute of Nuclear Science and Engineering for providing postgraduate research scholarship (PGRA 2016) to MA Alim is sincerely appreciated.

References

Author Manuscript

This article is protected by copyright. All rights reserved

1. A. Fujishima and K. Honda, "Electrochemical photolysis of water at a semiconductor electrode," *Nature*, 238[5358] 37-38 (1972).

2. O. Carp, C. L. Huisman, and A. Reller, "Photoinduced reactivity of titanium dioxide," *Prog. Solid State Chem.*, 32[1] 33-177 (2004).

3. M. Pelaez, N. T. Nolan, S. C. Pillai, M. K. Seery, P. Falaras, A. G. Kontos, P. S. M. Dunlop, J. W. J. Hamilton, J. A. Byrne, K. O'Shea, M. H. Entezari, and D. D. Dionysiou, "A review on the visible light active titanium dioxide photocatalysts for environmental applications," *Appl. Catal. B Environ.*, 125 331-49 (2012).

4. D. Dvoranová, V. Brezová, M. Mazúr, and M. A. Malati, "Investigations of metal-doped titanium dioxide photocatalysts," *Appl. Catal. B Environ.*, 37[2] 91-105 (2002).

5. T. Bak, J. Nowotny, N. J. Sucher, and E. Wachsman, "Effect of crystal imperfections on reactivity and photoreactivity of TiO_2 (rutile) with oxygen, water, and bacteria," *J. Phys. Chem. C*, 115[32] 15711-38 (2011).

6. T. Bak, W. Li, J. Nowotny, A. J. Atanacio, and J. Davis, "Photocatalytic properties of TiO_2: Evidence of the key role of surface active sites in water oxidation," *J. Phys. Chem. A*, 119[36] 9465-73 (2015).

7. W. Li, T. Bak, A. Atanacio, and J. Nowotny, "Photocatalytic properties of TiO_2: Effect of niobium and oxygen activity on partial water oxidation," *Appl. Catal. B Environ.* (2016). 198 243-53 (2016)

8. F. A. Kröger and H. J. Vink, "Relations between the concentrations of imperfections in crystalline solids," pp. 307-435. in Solid State Physics, Vol. Volume 3**.** Edited by S. Frederick and T. David. Academic Press, 1956.

9. J. Nowotny, "Oxide semiconductors for solar energy conversion: Titanium dioxide." CRC Press: Boca Raton, (2011).

10. P. Kofstad, "Nonstoichiometry, diffusion, and electrical conductivity in binary metal oxides." Wiley-Interscience New York, (1972).

11. M. Altomare, K. Lee, M. S. Killian, E. Selli, and P. Schmuki, "Ta-doped TiO_2 nanotubes for enhanced solar-light photoelectrochemical water splitting," *Chem. Eur. J*, 19[19] 5841-44 (2013).

Author Manuscript

This article is protected by copyright. All rights reserved

12. C. Visinescu, R. Sanjines, F. Levy, V. Marcu, and V. Parvulescu, "Tantalum doped titania photocatalysts: Preparation by dc reactive sputtering and catalytic behavior," *J. Photochem. Photobiol. A*, 174[2] 106-12 (2005).

13. H. Znad, M. H. Ang, and M. O. Tade, "Ta/TiO_2-and Nb/TiO_2-mixed oxides as efficient solar photocatalysts: Preparation, characterization, and photocatalytic activity," *Int. J. Photoenergy*, 2012 (2012).

14. K. Obata, H. Irie, and K. Hashimoto, "Enhanced photocatalytic activities of Ta, N co-doped TiO_2 thin films under visible light," *Chem. Phys.*, 339[1–3] 124-32 (2007).

15. L.-L. Tan, W.-J. Ong, S.-P. Chai, and A. R. Mohamed, "Visible-light-activated oxygen-rich TiO_2 as next generation photocatalyst: Importance of annealing temperature on the photoactivity toward reduction of carbon dioxide," *Chem. Eng. J.*, 283 1254-63 (2016).

16. G. R. Torres, T. Lindgren, J. Lu, C.-G. Granqvist, and S.-E. Lindquist, "Photoelectrochemical study of nitrogen-doped titanium dioxide for water oxidation," *J. Phys. Chem. B*, 108[19] 5995-6003 (2004).

17. J. Nowotny, M. A. Alim, T. Bak, M. A. Idris, M. Ionescu, K. Prince, M. Z. Sahdan, K. Sopian, M. A. M. Teridi, and W. Sigmund, "Defect chemistry and defect engineering of TiO_2-based semiconductors for solar energy conversion," *Chem. Soc. Rev.*, 44[23] 8424-42 (2015).

18. E. Tani and J. F. Baumard, "Electrical properties and defect structure of rutile slightly doped with Cr and Ta," *J. Solid State Chem.*, 32[1] 105-13 (1980).

19. J. F. Baumard and E. Tani, "Electrical conductivity and charge compensation in Nb doped TiO_2 rutile," *J. Chem. Phys.*, 67[3] 857-60 (1977).

20. J. F. Baumard and E. Tani, "Thermoelectric power in reduced pure and Nb-doped TiO_2 rutile at high temperature," *Phys. Status Solidi A*, 39[2] 373-82 (1977).

21. L. Sheppard, T. Bak, and J. Nowotny, "Electrical properties of niobium-doped titanium dioxide. 1. Defect disorder," *J. Phys. Chem. B*, 110[45] 22447-54 (2006).

22. J. Liu, H. Yang, W. Tan, X. Zhou, and Y. Lin, "Photovoltaic performance improvement of dye-sensitized solar cells based on tantalum-doped TiO_2 thin films," *Electrochim. Acta*, 56[1] 396-400 (2010).

Author Manuscript

This article is protected by copyright. All rights reserved

23. J.-H. Choi, S.-H. Kwon, Y.-K. Jeong, I. Kim, and K.-H. Kim, "Atomic layer deposition of Ta-doped TiO_2 electrodes for dye-sensitized solar cells," *J. Electrochem. Soc.*, 158[6] B749-B53 (2011).

24. U. Balachandran and N. G. Eror, "Self-compensation in tantalum-doped TiO_2," *J. Mater. Sci.*, 17[4] 1207-12 (1982).

25. E. Comini, M. Ferroni, V. Guidi, A. Vomiero, P. Merli, V. Morandi, M. Sacerdoti, G. Della Mea, and G. Sberveglieri, "Effects of Ta/Nb-doping on titania-based thin films for gas-sensing," *Sens. Actuator B-Chem.*, 108[1] 21-28 (2005).

26. D. Morris, Y. Dou, J. Rebane, C. Mitchell, R. Egdell, D. Law, A. Vittadini, and M. Casarin, "Photoemission and STM study of the electronic structure of Nb-doped TiO_2," *Phys. Rev. B*, 61[20] 13445 (2000).

27. W. Mertin, R. Gruehn, and H. Schäfer, "Neue beobachtungen zum system TiO_2-Ta_2O_5," *J. Solid State Chem.*, 1[3–4] 425-44 (1970).

28. J. Tauc, R. Grigorovici, and A. Vancu, "Optical properties and electronic structure of amorphous germanium," *Phys. Status Solidi B*, 15[2] 627-37 (1966).

29. P. Kubelka and F. Munk, " Ein beitrag zur potik der farbanstriche," *Z. Tech. Physik*, 12 593 (1931).

30. S. K. O'Leary and P. K. Lim, "On determining the optical gap associated with an amorphous semiconductor: A generalization of the Tauc model," *Solid State Commun.*, 104[1] 17-21 (1997).

31. M. K. Nowotny, T. Bak, and J. Nowotny, "Electrical properties and defect chemistry of TiO_2 single crystal. I. Electrical conductivity," *J. Phys. Chem. B*, 110[33] 16270-82 (2006).

32. L. R. Sheppard, M. K. Nowotny, T. Bak, and J. Nowotny, "Effect of cooling on electrical conductivity of TiO_2," *Phys. Status Solidi B*, 245[9] 1816-27 (2008).

Author Manuscript

Table 1. Defect equilibria, the related equilibrium constants and the associated standard enthalpy and entropy of defect formation (n and p represent the concentration of electrons and electron holes, respectively, and square brackets denote concentrations)

This article is protected by copyright. All rights reserved

	Defect reaction	Equilibrium constant	ΔH^O kJ/mol	ΔS^O J/(mol.K)
1	$O_O^x \Leftrightarrow V_O^{\bullet\bullet} + 2e' + ½O_2$	$K_1 = [V_O^{\bullet\bullet}]n^2p(O_2)^{1/2}$	493.1	106.5
2	$Ti_{Ti}^x + 2O_O^x \Leftrightarrow Ti_i^{\bullet\bullet\bullet} + 3e' + O_2$	$K_2 = [Ti_i^{\bullet\bullet\bullet}]n^3p(O_2)$	879.2	190.8
3	$Ti_{Ti}^x + 2O_O^x \Leftrightarrow Ti_i^{\bullet\bullet\bullet\bullet} + 4e' + O_2$	$K_3 = [Ti_i^{\bullet\bullet\bullet\bullet}]n^4p(O_2)$	1025.8	238.3
4	$O_2 \Leftrightarrow V_{Ti}'''' + 4h^\bullet + 2O_O^x$	$K_4 = [V_{Ti}'''']p^4p(O_2)^{-1}$	354.5	-202.1
5	$nil \Leftrightarrow e' + h^\bullet$	$K_i = np$	222.1	-44.6
		$\mathbf{lnK} = [(\Delta \mathbf{S^o})/\mathbf{R}] - [(\Delta \mathbf{H^o})/\mathbf{RT}]$		

Table 2. The concentration of the elements determined by the PIXE analysis, including the element incorporated intentionally (tantalum) and not-intentionally (contaminations).

Species	At %
Cl	0.12
K	0.006
Ti	59.82
Fe	0.03
Ni	0.07
Zn	0.004
Ta	**0.39**

Figure captions

Figure 1. The Brouwer-type diagram for Ta-doped TiO_2 showing defect disorder within different ranges of oxygen activity (where square brackets denote concentrations and the fraction numbers are represented by Equation (8)

Author Manuscript

This article is protected by copyright. All rights reserved

Figure 2. Schematic representation of the effect of oxygen activity on the concentration of electrons (a), electrical conductivity (b) and thermoelectric power (S) for donor-doped TiO_2, where D is a donor-type ion (c), the fractions are related to the oxygen activity-related exponent for specific quantities represented by Equations (8), (10) and (18), respectively

Figure 3. Schematic representation of the effect of oxygen activity for pure and Nb-doped TiO_2 in reducing and strongly reducing conditions [19-20]

Figure 4. The SEM micrographs for (a) pure TiO_2, (b) Ta-doped TiO_2 specimen after polishing and subsequent annealing at 1273 K for 2 h and (c) Ta-doped TiO_2 specimen after all oxidation and reduction runs associated with the electrical conductivity measurements - magnification of 2000

Figure 5. The PIXE spectra for pure and the Ta-doped TiO_2 (the peaks are related to the indicated elements)

Figure 6. Effect of tantalum concentration on the band gap

Figure 7. A schematic representation of experimental set-up for the determination of the electrical conductivity using the four probe method (appropriate wiring was provided for the electrical monitoring devices, which were located outside the high temperature area)

Figure 8. The monitoring sheet involving the changes of oxygen activity (a), temperature (b) and the electrical conductivity as a function of time within a single step of the reduction experiment for Ta-doped TiO_2 at 1173 K

Figure 9. Isothermal changes of (a) the electrical conductivity, (b) thermoelectric power and (c) oxygen activity as a function of time for Ta-doped TiO_2 at 1273 K

Figure 10. Electrical conductivity of Ta-doped TiO_2 (0.39 at. %) as a function of oxygen activity in the temperature range 1173 – 1323 K (dashed lines are the extrapolated dependences)

Figure 11. The effect of oxygen activity on the electrical conductivity for pure and Ta-doped TiO_2 (plotted along Nb-doped TiO_2) at (a) 1173 K (the plot for Nb-doped TiO_2 corresponds to 1198 K), 1223 K (b), 1273 K (c) and 1323 K (d)

Figure 12. Effect of oxygen activity on the electrical conductivity of Ta-doped TiO_2 at 1273 K obtained in this work along the data reported by Tani and Baumard [18]

Figure 13. The isothermal dependences of the thermoelectric power as a function of oxygen activity for Ta-doped TiO_2 in the range 1173 K – 1323 K

Figure 14. Effect of oxygen on the Fermi level of pure and Ta-doped TiO_2 at 1323 K

Figure 15. Isobaric Arrhenius plots for Ta-doped TiO_2 in reducing and oxidising conditions

Author Manuscript

This article is protected by copyright. All rights reserved

Figure 16. Effect of oxygen activity on the activation energy of electrical conductivity

Figure 17. The effect of oxygen activity on the enthalpy of defect formation of TiO_2

Author Manuscript

This article is protected by copyright. All rights reserved

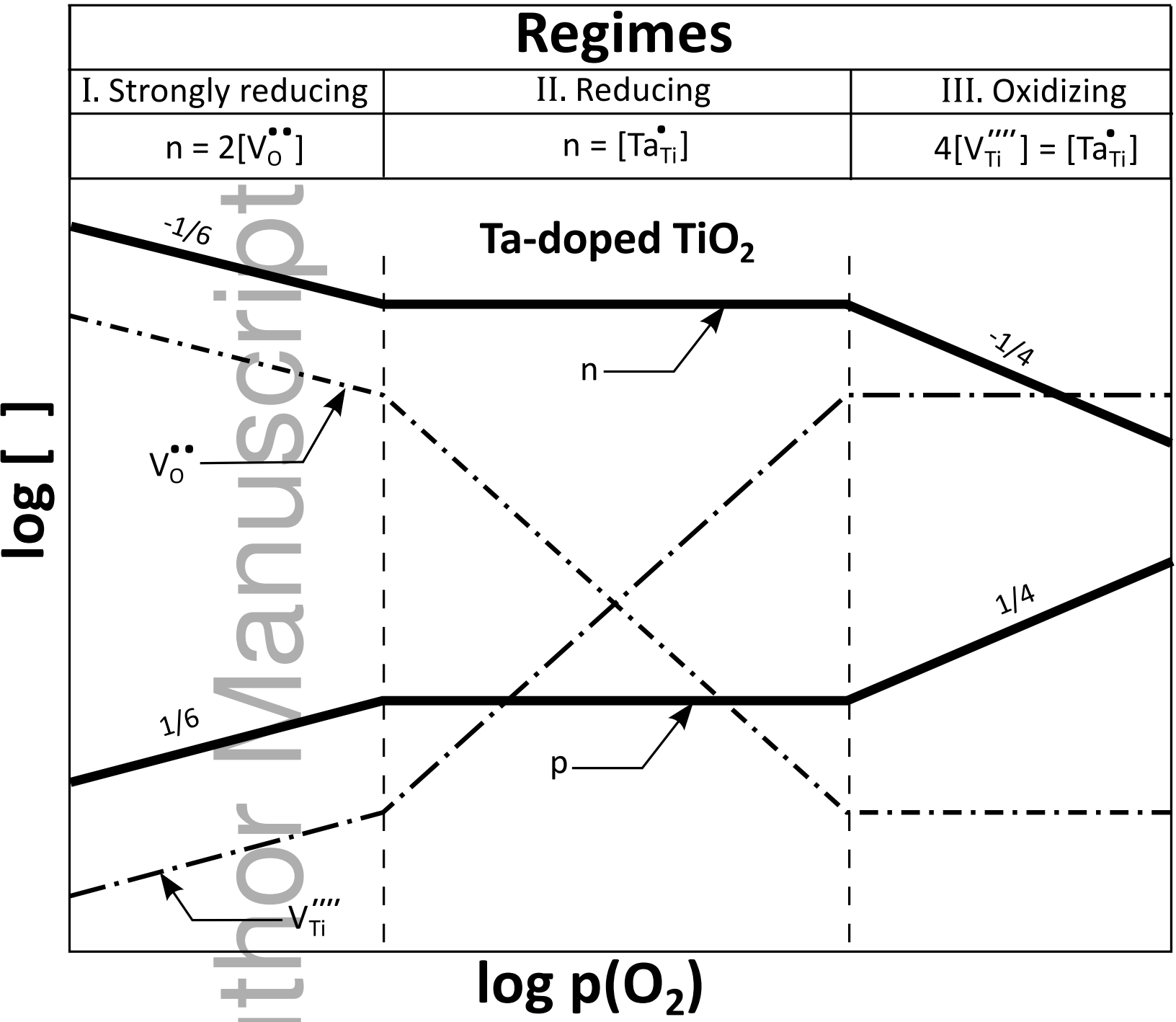

jace_14959_f1.eps

Author Manuscript

This article is protected by copyright. All rights reserved

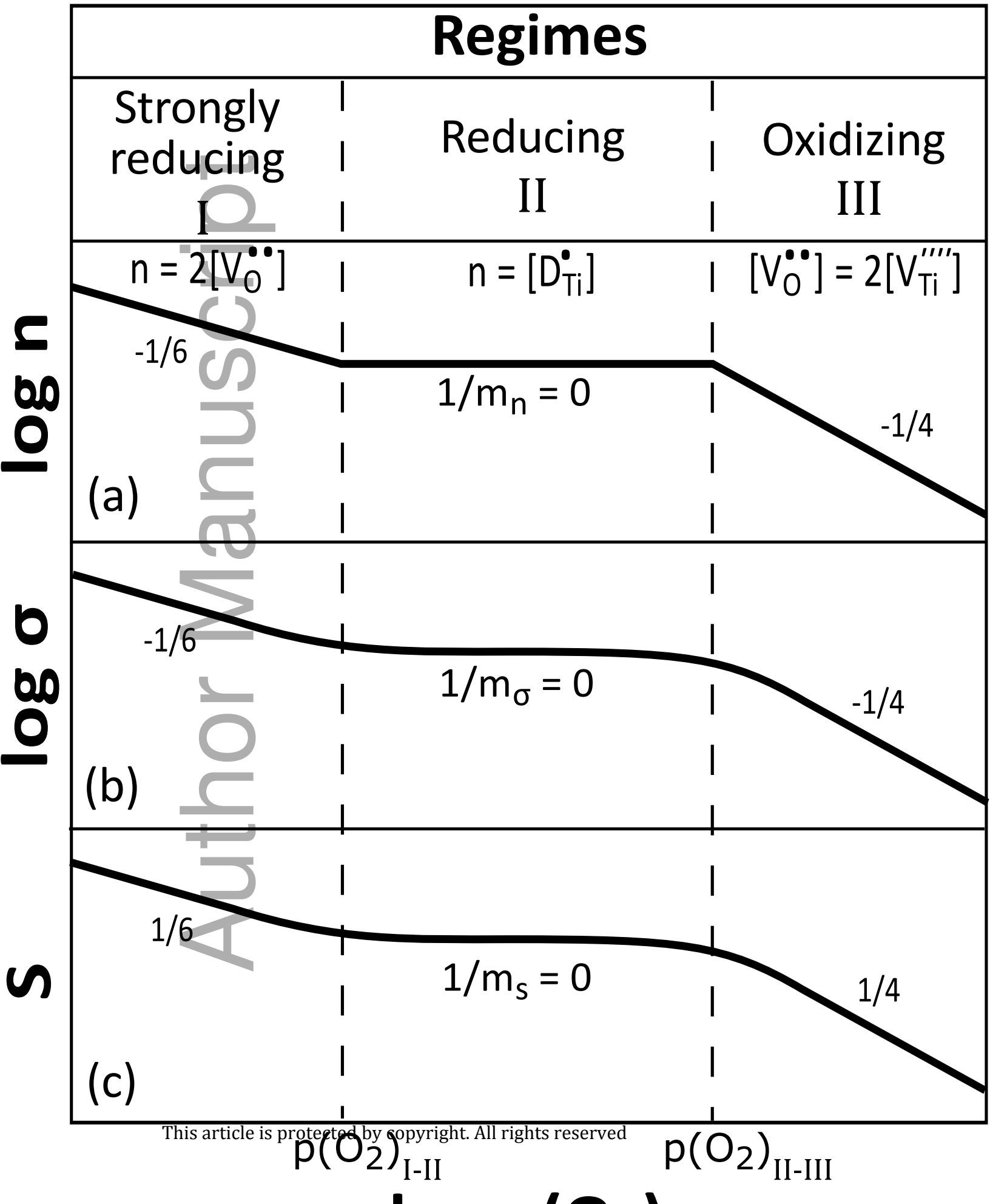

Author Manuscript

This article is protected by copyright. All rights reserved

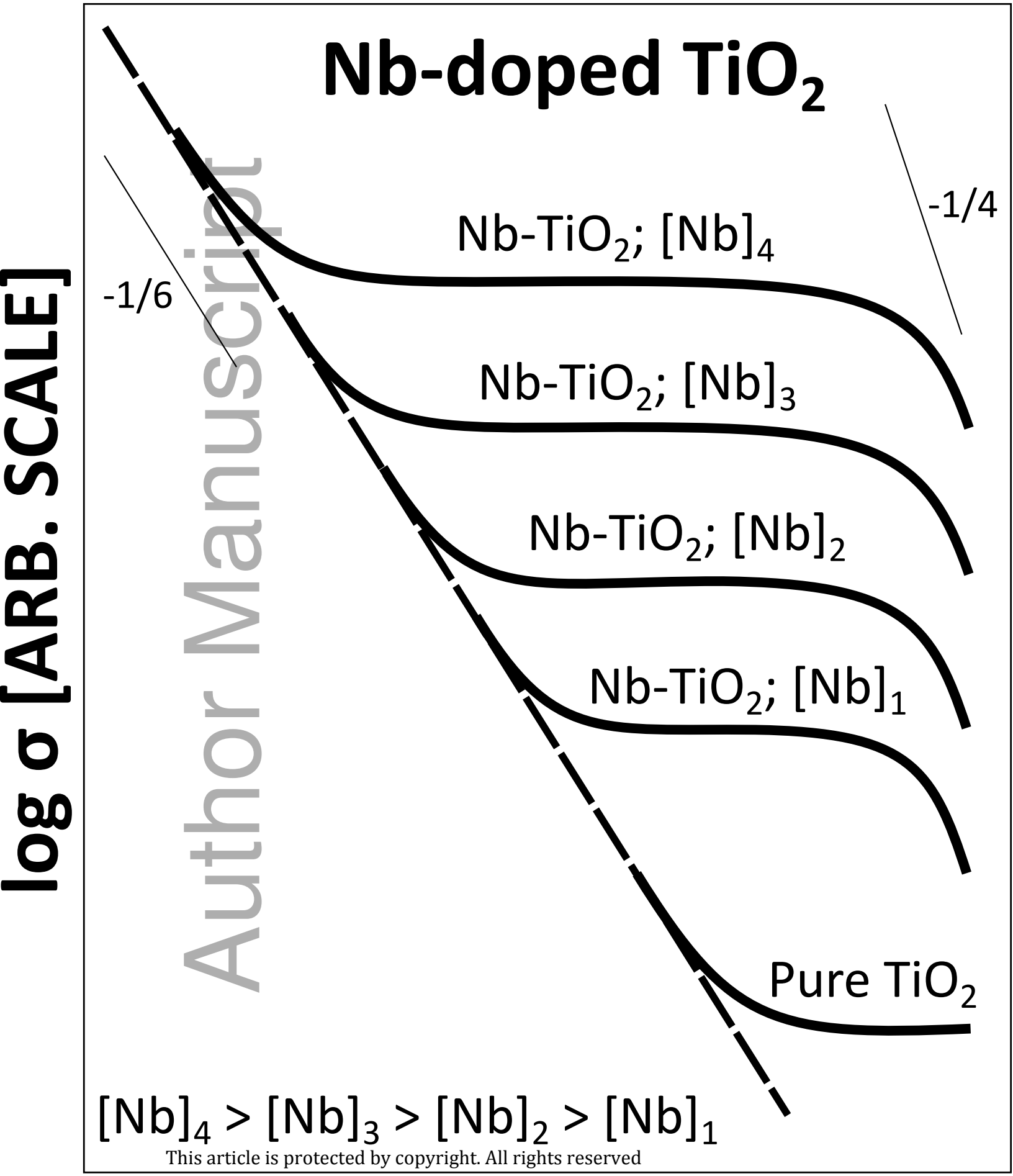

Author Manuscript

This article is protected by copyright. All rights reserved

Author Manuscript

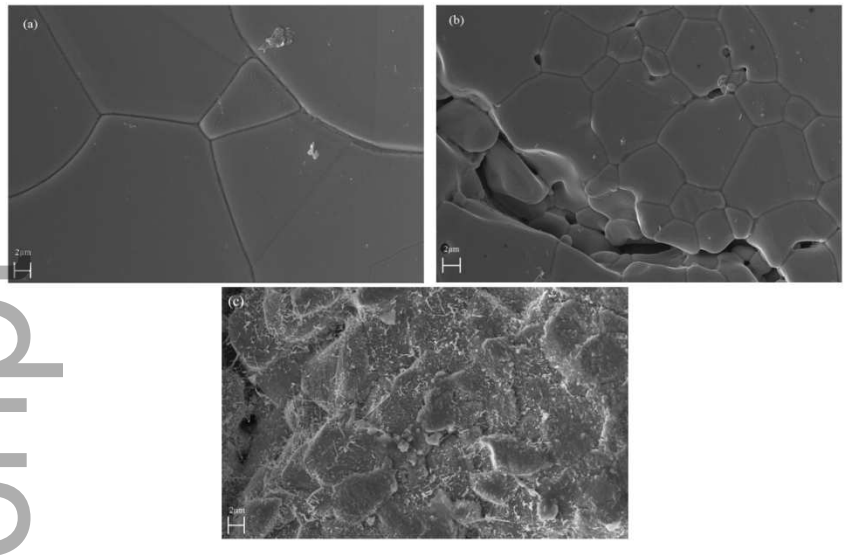

jace_14959_f4.tif

This article is protected by copyright. All rights reserved

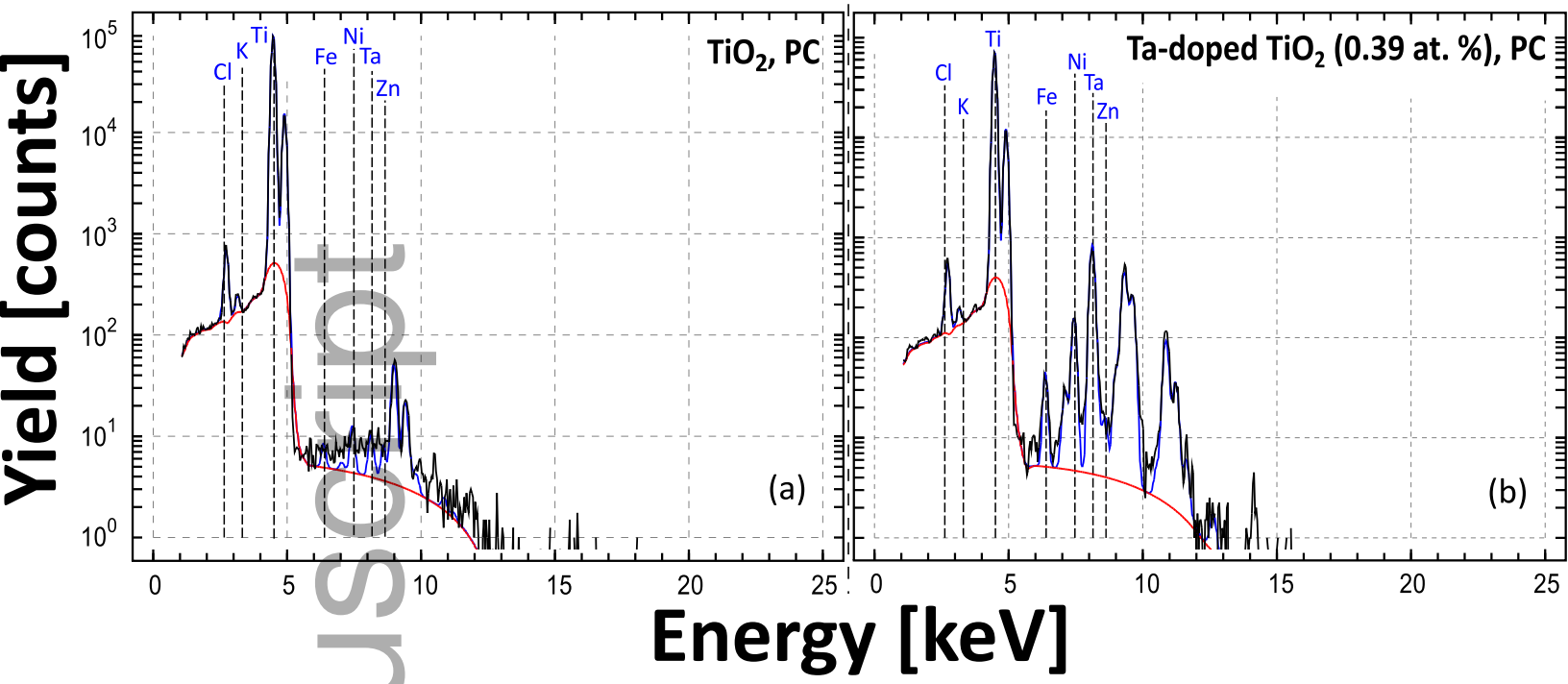

jace_14959_f5.eps

Author Manuscript

This article is protected by copyright. All rights reserved

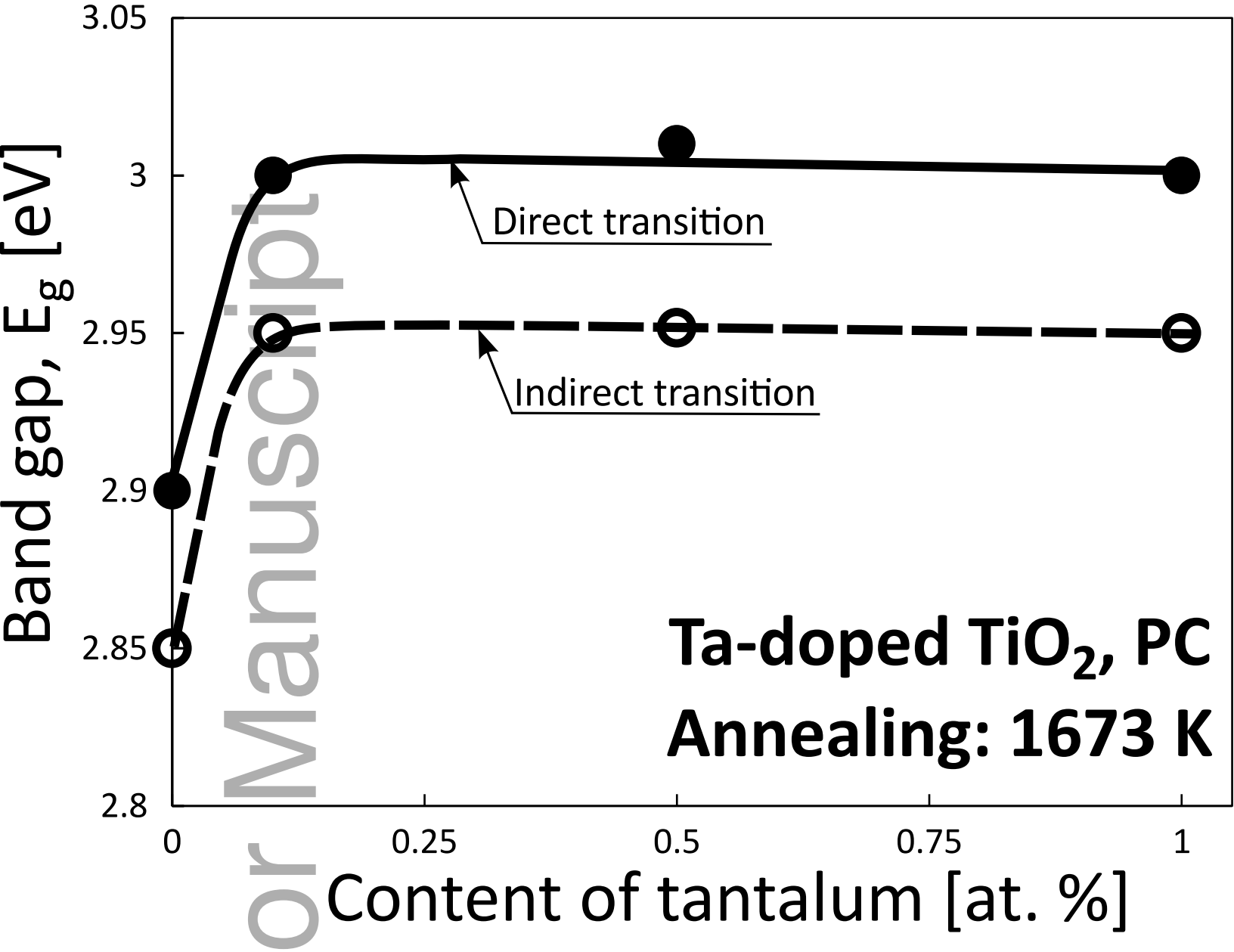

jace_14959_f6.eps

Author Manuscript

This article is protected by copyright. All rights reserved

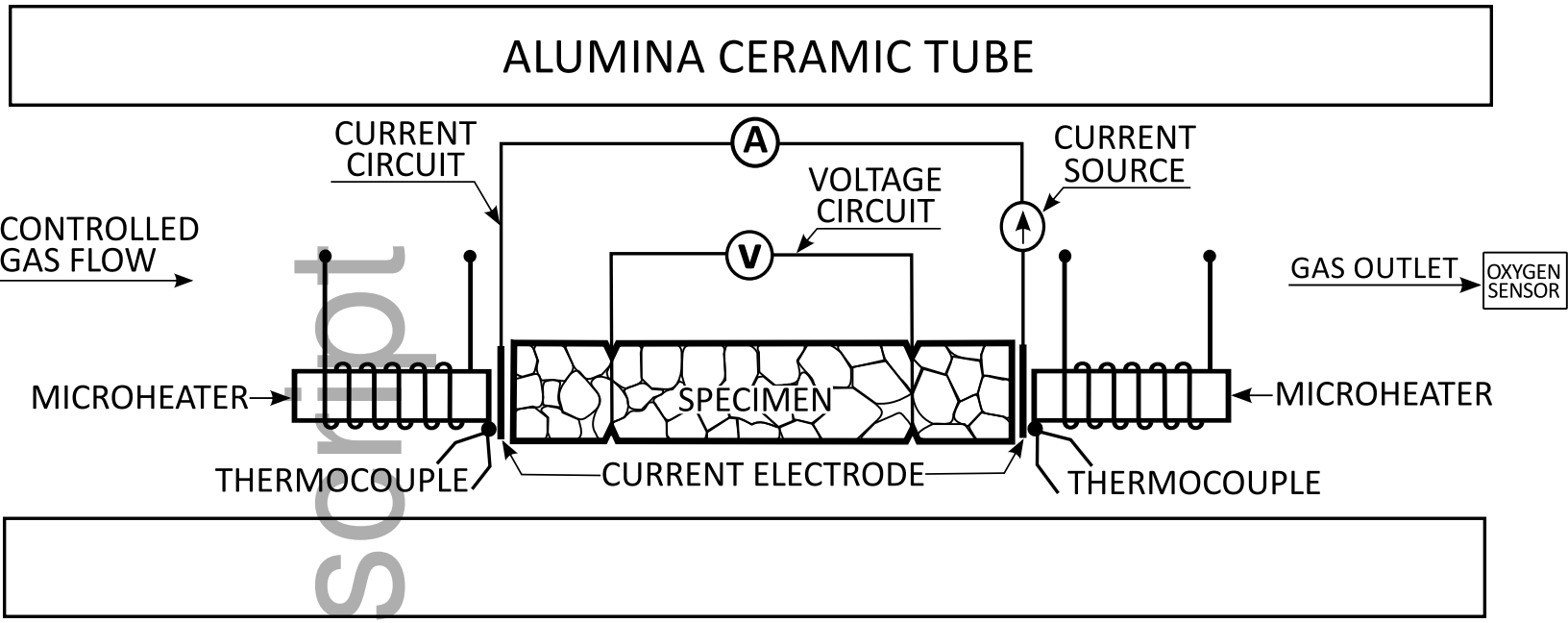

jace_14959_f7.eps

Author Manuscript

This article is protected by copyright. All rights reserved

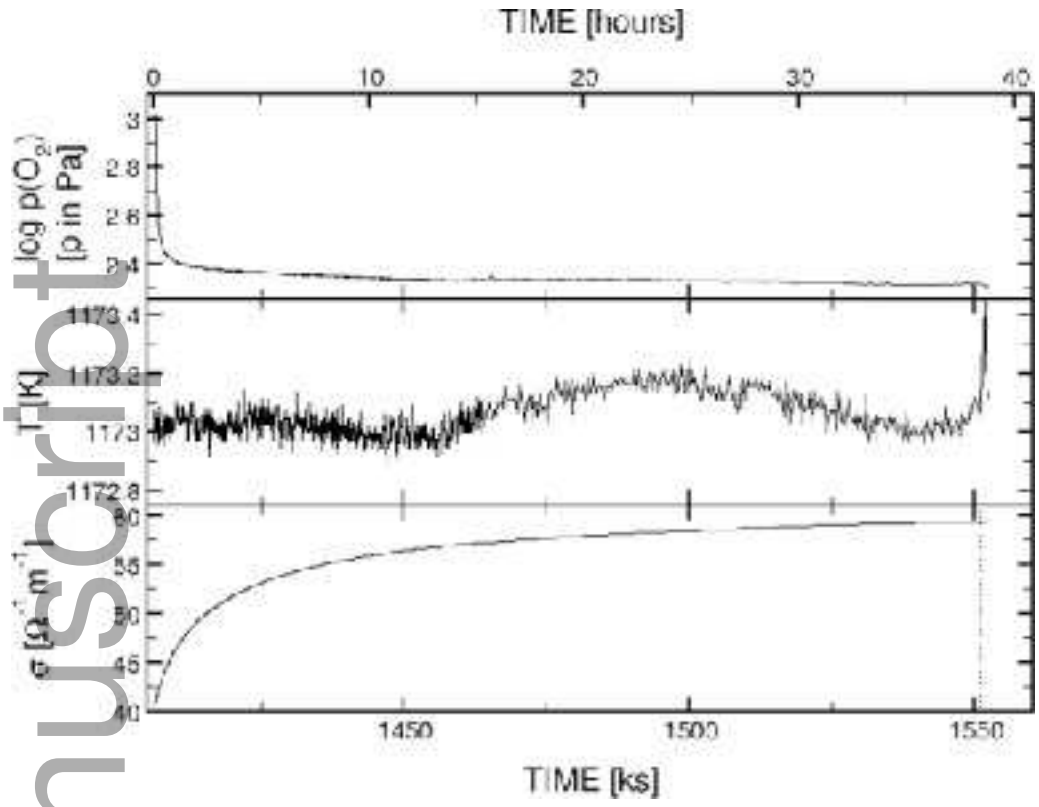

jace_14959_f8.tif

Author Manuscript

This article is protected by copyright. All rights reserved

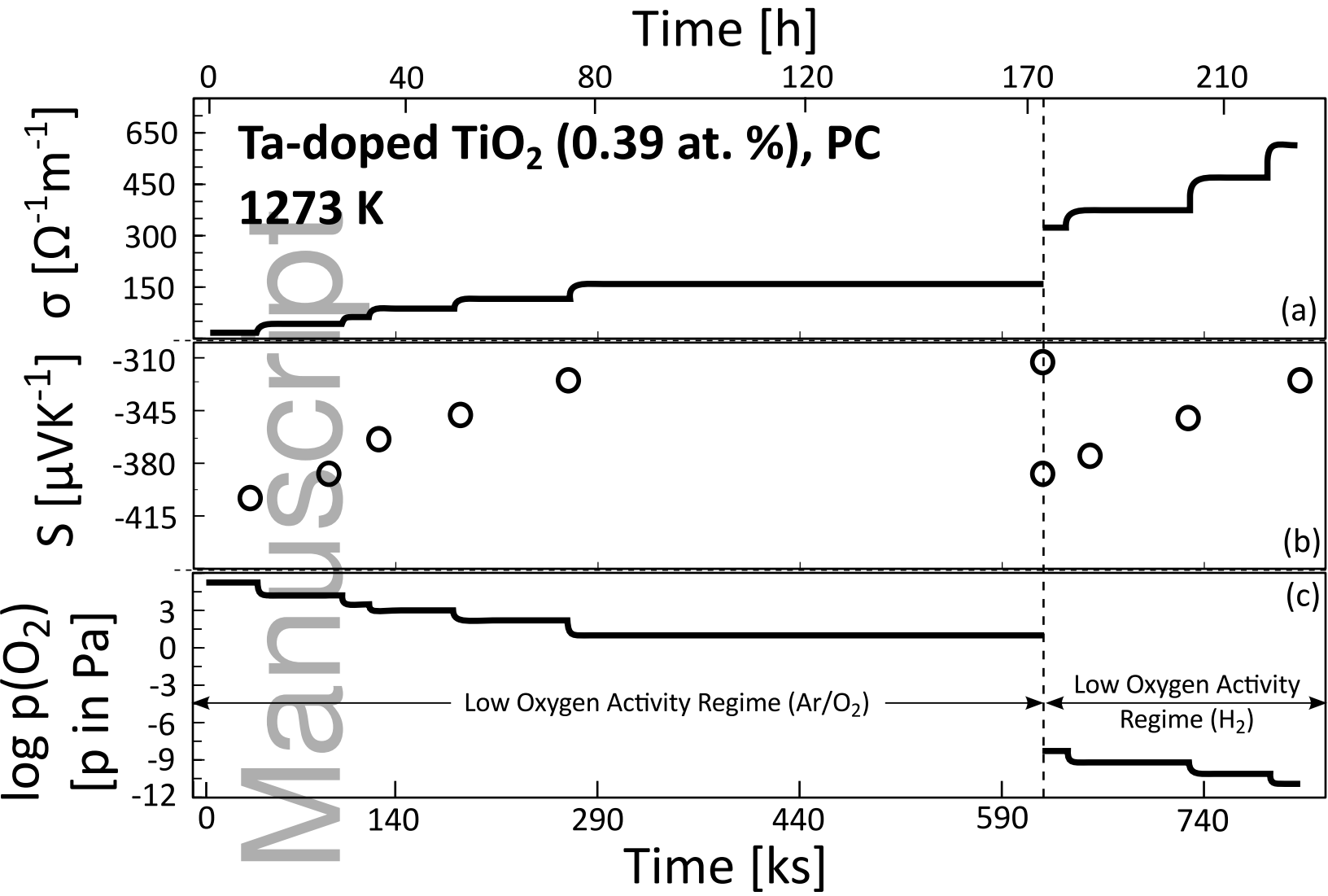

jace_14959_f9.eps

Author Manuscript

This article is protected by copyright. All rights reserved

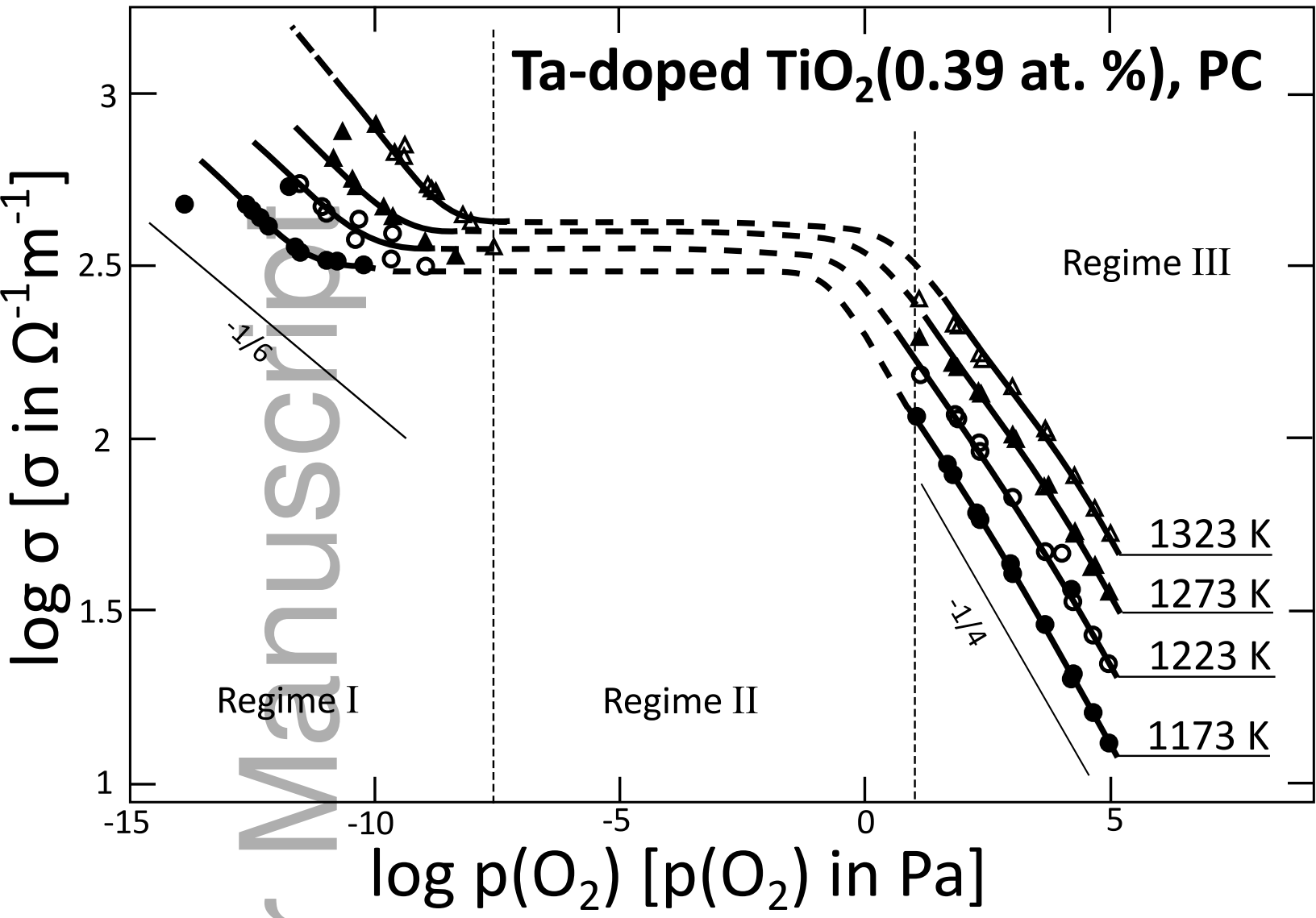

jace_14959_f10.eps

Author Manuscript

This article is protected by copyright. All rights reserved

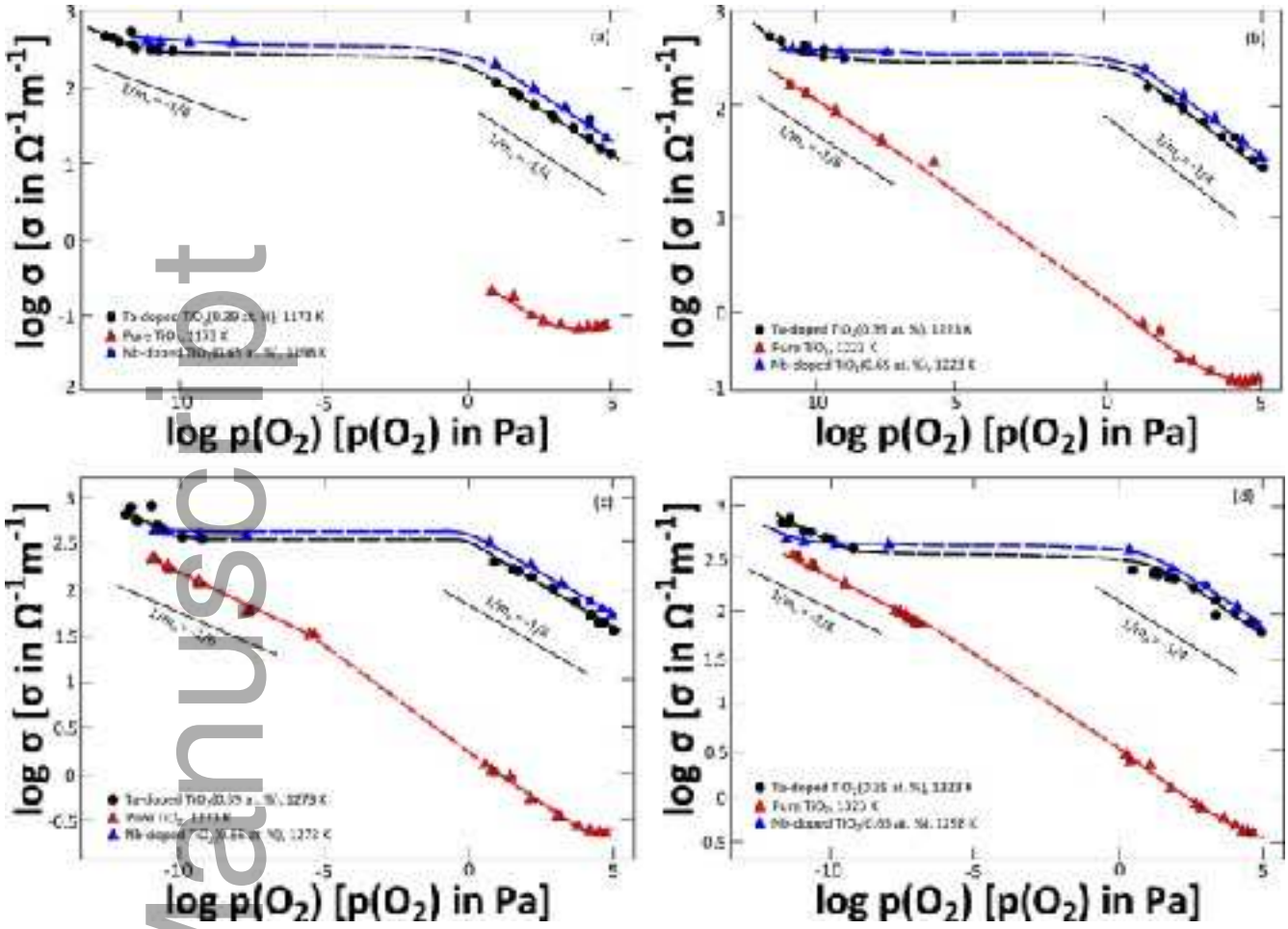

jace_14959_f11.tif

Author Manuscript

This article is protected by copyright. All rights reserved

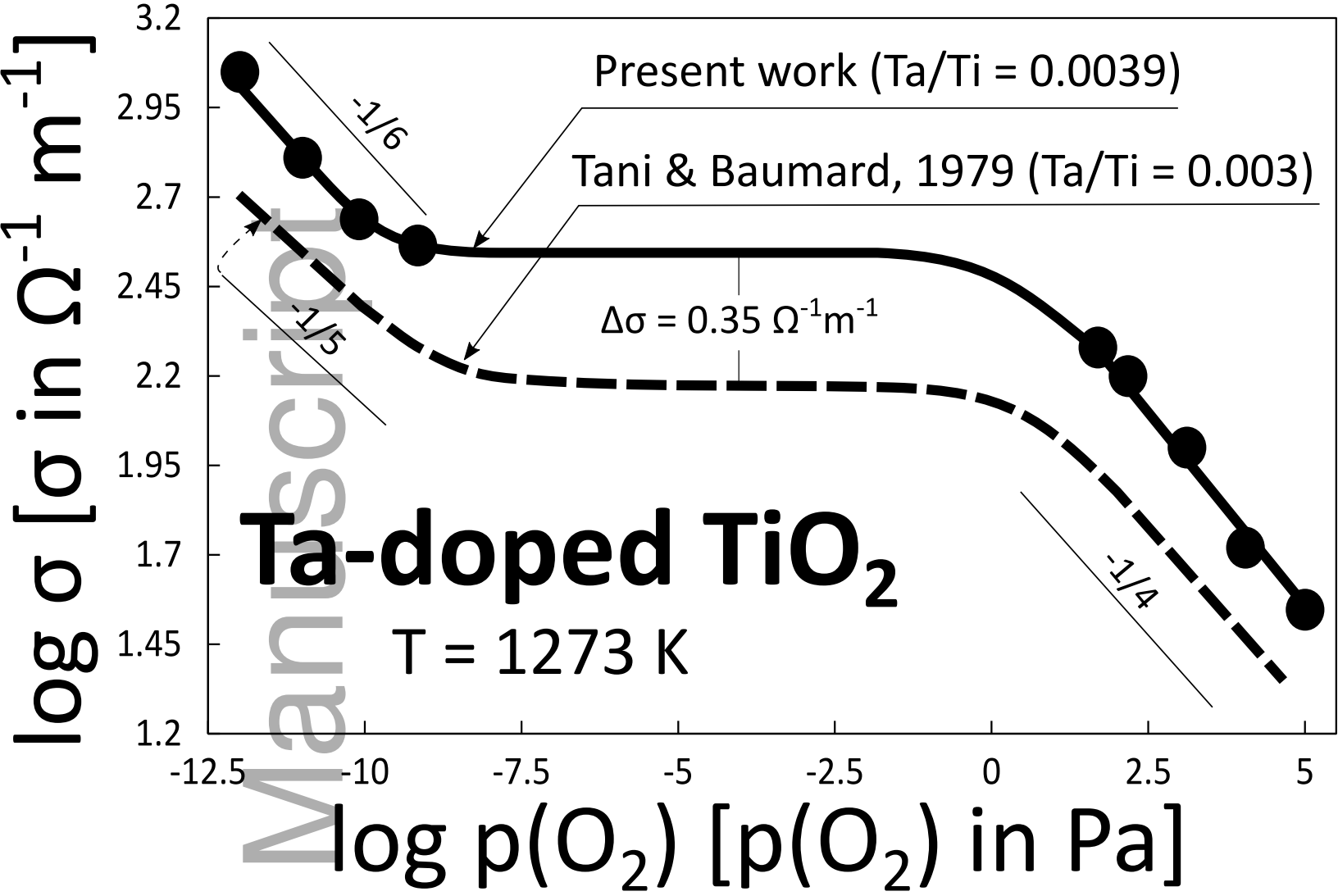

jace_14959_f12.eps

Author Manuscript

This article is protected by copyright. All rights reserved

jace_14959_f13.eps

Author Manuscript

This article is protected by copyright. All rights reserved

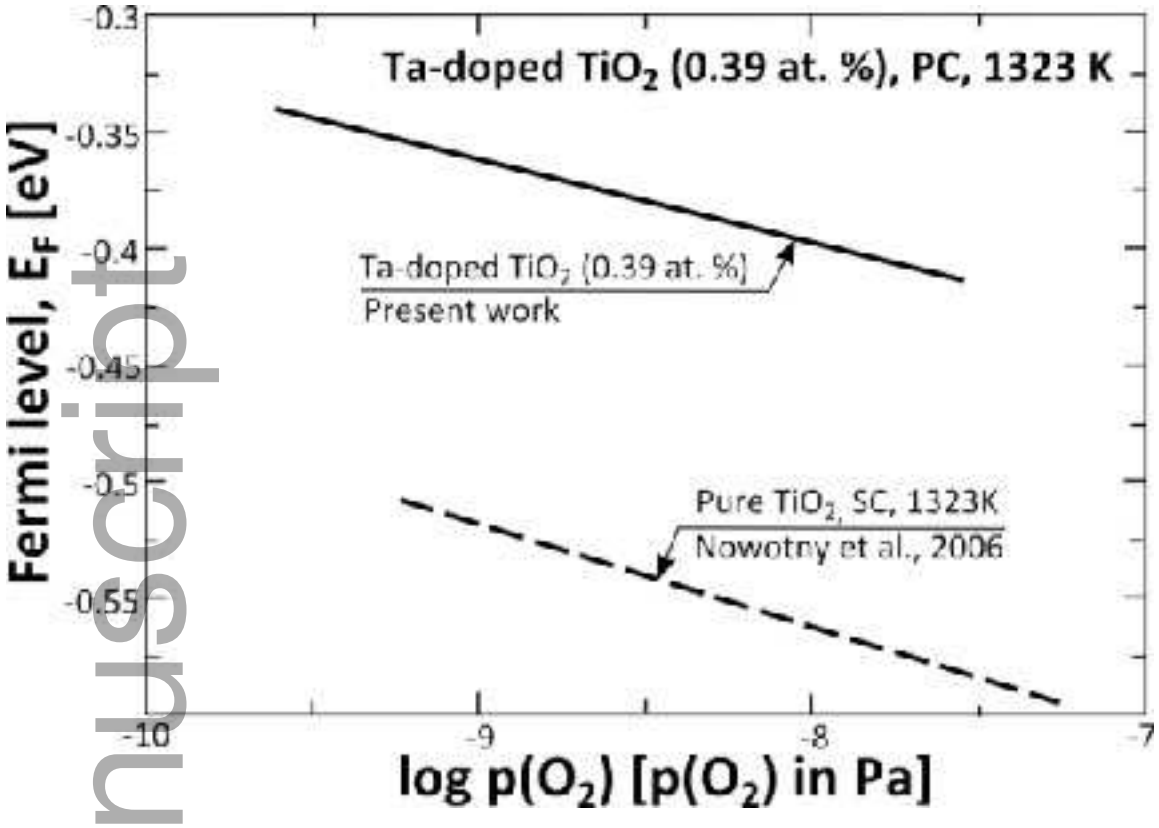

jace_14959_f14.tif

Author Manuscript

This article is protected by copyright. All rights reserved

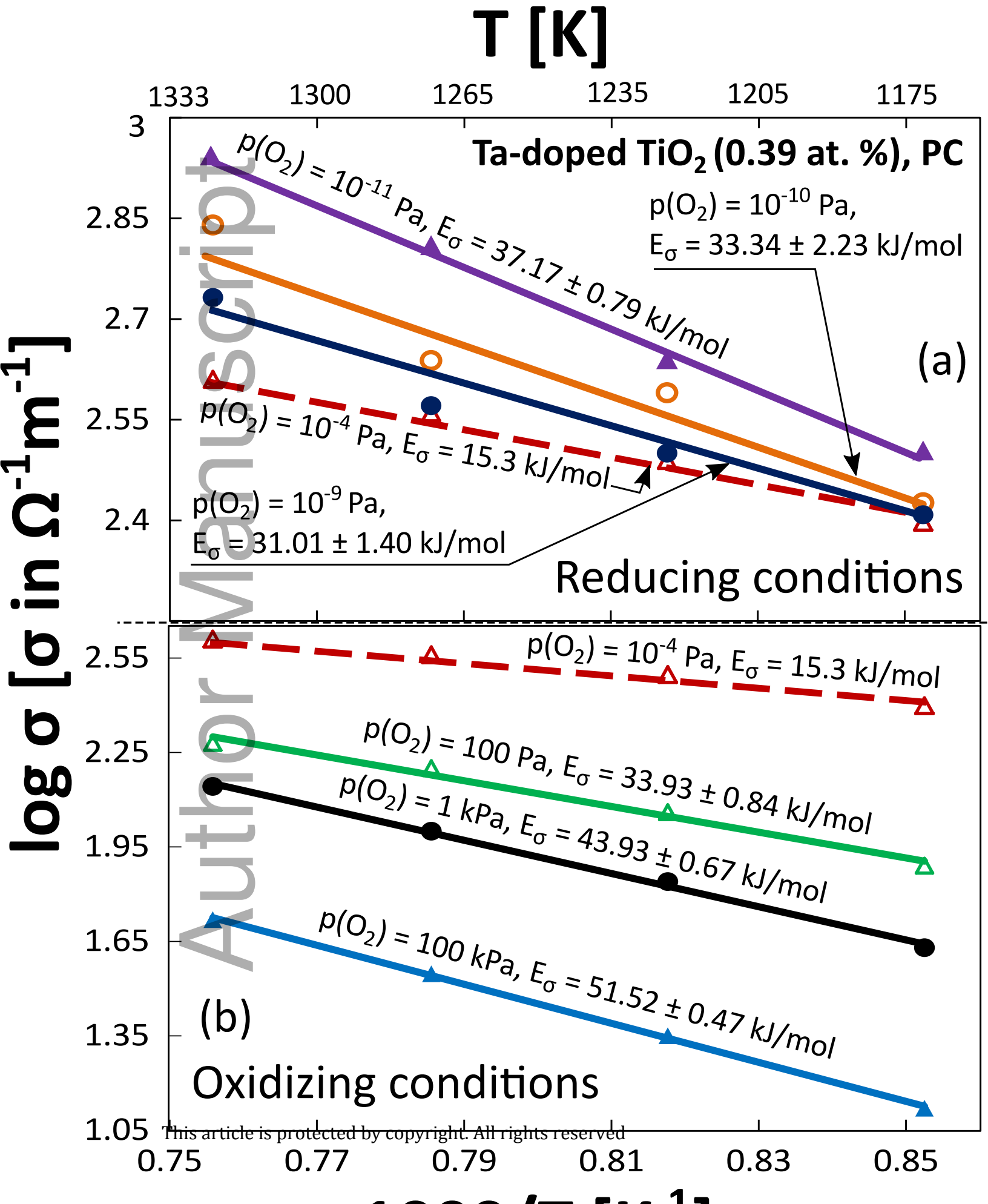

Author Manuscript

This article is protected by copyright. All rights reserved

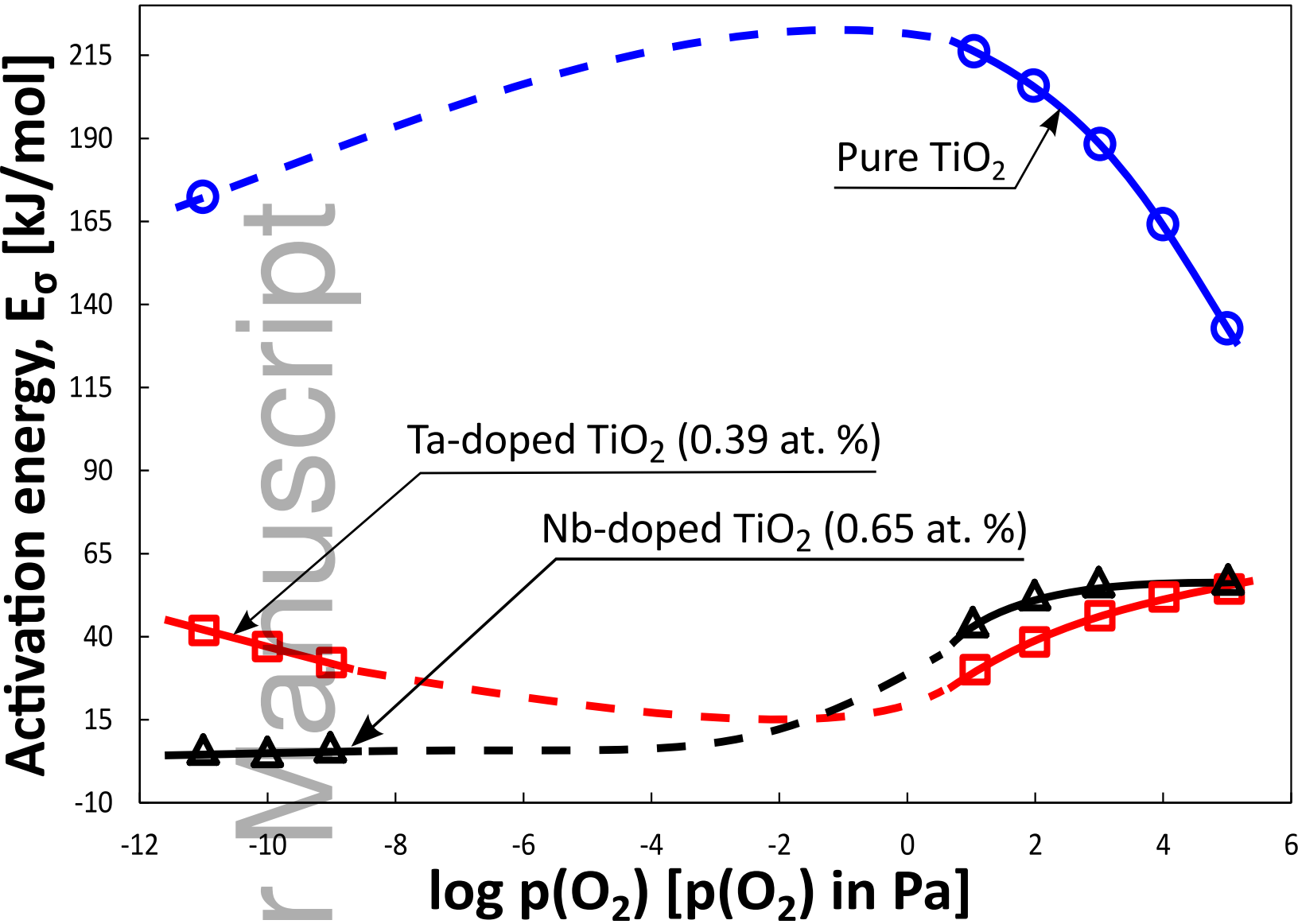

jace_14959_f16.eps

Author Manuscript

This article is protected by copyright. All rights reserved

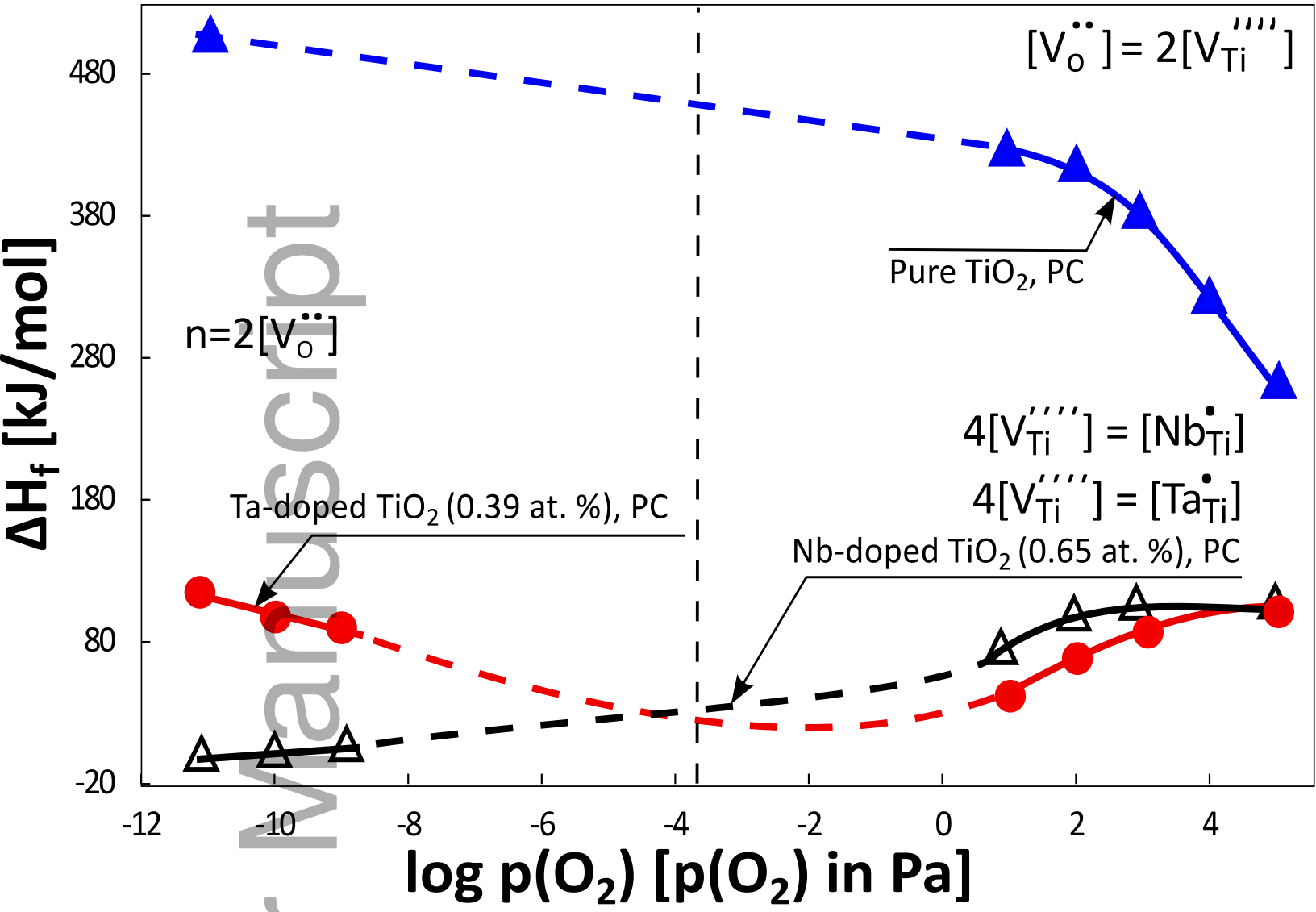

jace_14959_f17.eps

Author Manuscript

This article is protected by copyright. All rights reserved

University Library

MINERVA ACCESS

A gateway to Melbourne's research publications

Minerva Access is the Institutional Repository of The University of Melbourne

Author/s:
Alim, MA;Bak, T;Atanacio, A;Du Plessis, J;Zhou, M;Davis, J;Nowotny, J

Title:
Electrical conductivity and defect disorder of tantalum-doped TiO2

Date:
2017-09-01

Citation:
Alim, M. A., Bak, T., Atanacio, A., Du Plessis, J., Zhou, M., Davis, J. & Nowotny, J. (2017). Electrical conductivity and defect disorder of tantalum-doped TiO2. Journal of the American Ceramic Society, 100 (9), pp.4088-4100. https://doi.org/10.1111/jace.14959.

Persistent Link:
http://hdl.handle.net/11343/292945